

# Analysis of bearing capacity of aluminum alloy box girder after welding

Dengrong Yu<sup>a\*</sup>, Jiancong Chao<sup>b</sup>

<sup>a</sup>Zhuhai Xianghai Bridge Co., Ltd, Zhuhai 519060, Guangdong, China; <sup>b</sup>School of Civil Engineering, Chongqing Jiaotong University, Chongqing 400074, China

## ABSTRACT

In order to study the influence of welding on the aluminum alloy box girder, the welding temperature field of the aluminum alloy box girder was simulated by using the finite element software Abaqus, and then the stress change of each plate of the aluminum alloy box girder during the welding process was analyzed. The results show that the bearing capacity of the aluminum alloy box girder is reduced by 24.94% by welding, and the bearing capacity of the steel box girder is reduced by 16.67% under the same conditions, indicating that the impact of welding on the aluminum alloy box girder is more obvious. When the aluminum alloy box girder reaches the ultimate bearing capacity, the failure mode is the same as that of the steel box girder, that is, bending failure.

**Keywords:** Aluminum alloy box girder, welding analysis, load displacement curve, failure mechanism

## 1. INTRODUCTION

As an infrastructure that crosses valleys and rivers and connects the transportation between the two places, bridges play an extremely important role in transportation. In the process of industrial development, aluminum alloy materials are gradually applied to the bridge field with their light weight and high strength. The aluminum alloy-concrete composite simply supported box girder is different from the truss bridge. The truss bridge is spliced by many aluminum alloy rods, these rods are often extruded, and the size of the aluminum alloy box girder is larger, there is no such huge die-casting equipment on the market for the time being, so it is necessary to weld and connect the plates of the aluminum alloy girder.

In 1989, Ueda<sup>1</sup> of Osaka University in Japan proposed the intrinsic strain method, which believed that the deformation of welded structures is mainly due to intrinsic strain, and that the intrinsic strain can be obtained by empirical formulas, experimental measurements, thermoselastoplastic analysis, etc. In 1992, Ueda et al.<sup>2</sup> used numerical simulation to study the influence of various influencing factors, including assembly and welding sequence, initial stress, and assembly clearance, on structural deformation. In 1999, Bachorski et al.<sup>3</sup> from Australia analyzed the weld deformation of butt joints by linear elastic volume shrinkage method, and concluded that the deformation of the joint angle increased with the increase of the inner angle of the unilateral fracture of the joint. In 2006, Zhang et al.<sup>4</sup> from the University of Pennsylvania proposed the concept of the “Applied Plastic Strain Method”, which showed that this algorithm has certain advantages in accurately predicting the twisting and bending deformation of structures. In 2007, Deng et al.<sup>5</sup> from the Computational Mechanics Research Center in Japan used the elastic finite element method to predict the welding deformation based on the intrinsic strain theory, and verified the effectiveness of the proposed elastic finite element method. In 2011, Sulaiman et al.<sup>6</sup> from Malaysia used weld planner software to study the weld deformation analysis of diagonal joints and butt joints, and compared the results of numerical simulation with the actual measurement results, thus proving the feasibility of weld planner software in welding deformation analysis. In 2015, Chen et al.<sup>7</sup> carried out a finite element simulation of the structure of the marine stiffener of a large structure, and simplified and optimized the structure in the form of shell elements, and found that the welding sequence has a great influence on the residual stress and deformation of the stiffener after welding. Bhatti et al.<sup>8</sup> used the thermoelastoplastic finite element method to study the influence mechanism of thermodynamic physical parameters on welding residual stress and deformation of high-strength steel. In 2016, Huang et al.<sup>9</sup> used a local solid model and a global shell model to quickly predict the deformation of laser-welded thin plates based on the intrinsic strain theory. The transient thermoselastoplastic analysis of the local 3D solid model was carried out, and the predicted deformation mode and deformation amplitude were consistent with the measured results.

\*22284676@qq.com

Based on the existing theory and design specifications of steel-concrete composite beams, this paper proposes an aluminum alloy simply supported box girder. Taking the 5m span of the new simply supported girder as the research object, the welding process of the aluminum alloy box girder is simulated by Abaqus, and the distribution of residual stress after welding of the aluminum alloy box girder can be obtained. At the same time, the effect of residual stress after welding on the bearing capacity of aluminum alloy box girder was explored.

## 2. FINITE ELEMENT ANALYSIS OF WELDING IN ALUMINUM ALLOY BOX GIRDERS

The main body of the box girder uses 6082-T6 aluminum alloy material, and the welds are filled with ER5356. When the welding speed is 5mm/s, the residual stress is minimal, hence the welding speed is set at 5 mm/s with a total welding duration of 100s and post-weld cooling of 10000s. Taking about 50s into the welding process as an example, the welding temperature field distribution cloud diagrams are extracted as shown in the Figure 1. For ease of comparison, a similarly sized steel box girder model is established.

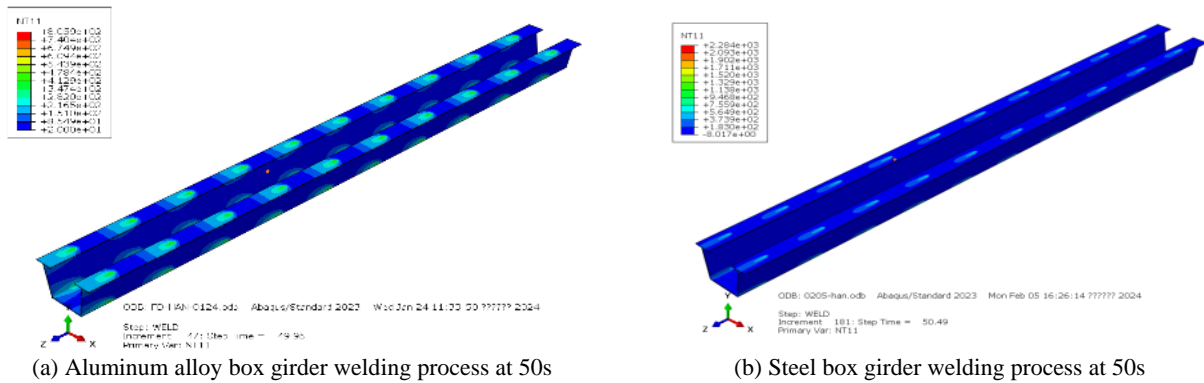


Figure 1. Welding temperature field of different box girder.

From the comparison, it is evident that during the welding process, the temperature influence range of the aluminum alloy box girder is greater than that of the steel box girder. This is because the thermal conductivity of aluminum alloy material is high, approximately twice that of steel, leading to fast heat transfer and loss. As the welding process progresses, with the continuous input of heat at the source location, the temperature in the weld zone keeps rising, eventually reaching the material's melting point, causing the material to melt and form a molten pool, the shape of which is illustrated in the Figure 2.

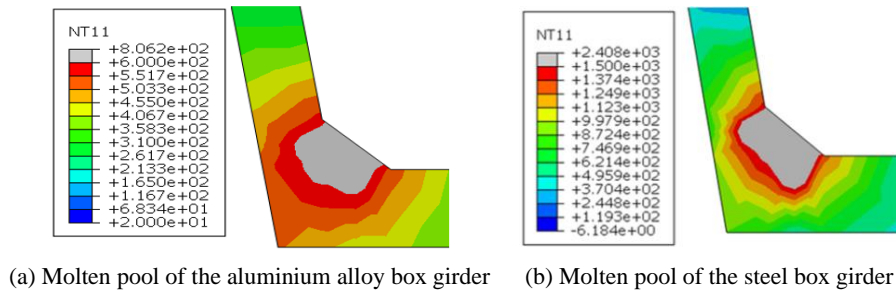


Figure 2. Welding temperature field of different box girder.

## 3. POST-WELD LOAD-BEARING CAPACITY CALCULATION

The load-bearing capacity calculation model in this section utilizes C3D8R solid elements with a mesh size of 10mm × 10mm. The loading method is the same as in Chapter 2, setting four sets of models for comparison: A and B are steel box girders, C and D are aluminum alloy box girders. Groups A and C do not consider residual welding stresses, whereas groups B and D do. The loading method is mid-span loading, and end plates are installed at the supports to prevent shearing damage.

The load-displacement curves for A, B, C, and D are obtained as shown in Figure 3. Without considering residual stress, A's ultimate load-bearing capacity is about 421.60 kN, while C's ultimate load-bearing capacity is 342.78 kN. Under the same structural dimensions, C's capacity is about 81.3% of A's capacity. With the influence of residual stress, the ultimate load-bearing capacities of B and D decrease: B's capacity drops to about 356.76 kN (a 16.67% decrease from A), and D's capacity to about 255.29 kN (a 24.94% decrease from C), which is a more significant reduction by about 1.57 times that of the steel girder. Thus, it is evident that welding residual stress has a greater impact on the load-bearing capacity of aluminum alloy box girders compared to steel girders.

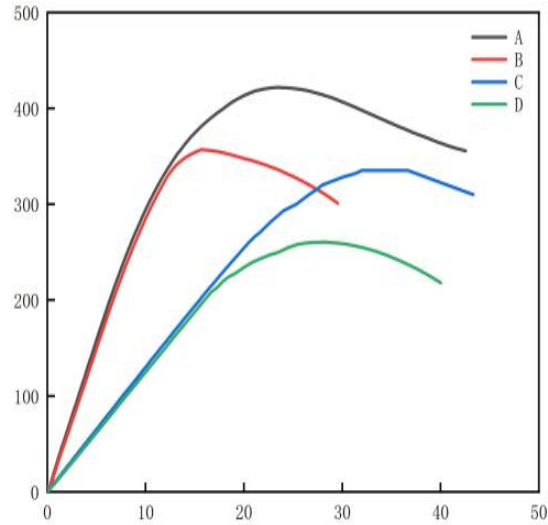
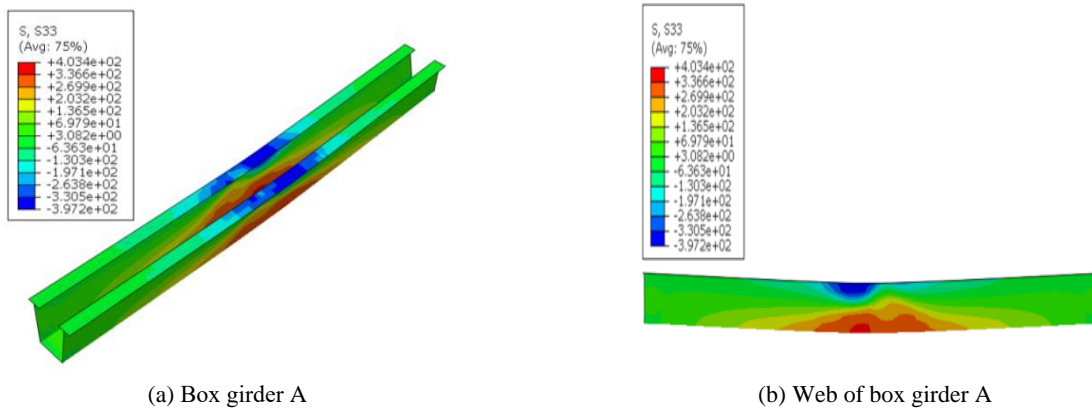


Figure 3. Comparative for load-displacement curves.

The destruction states of A, B, C, and D after reaching their ultimate load-bearing capacities are extracted as shown in the Figure 4. The comparison shows that the failure modes under the influence of residual stresses are similar to those without considering residual stresses, characterized by bending failure. The top and bottom plates of the box girders exceed the material's yield strength. Observations show significant increases in tensile stress around the bottom plate welds, reaching the material's yield strength. Near the weld areas of the steel girder's top plate, the closer to the mid-span, the smaller the tensile stress.



(a) Box girder A

(b) Web of box girder A

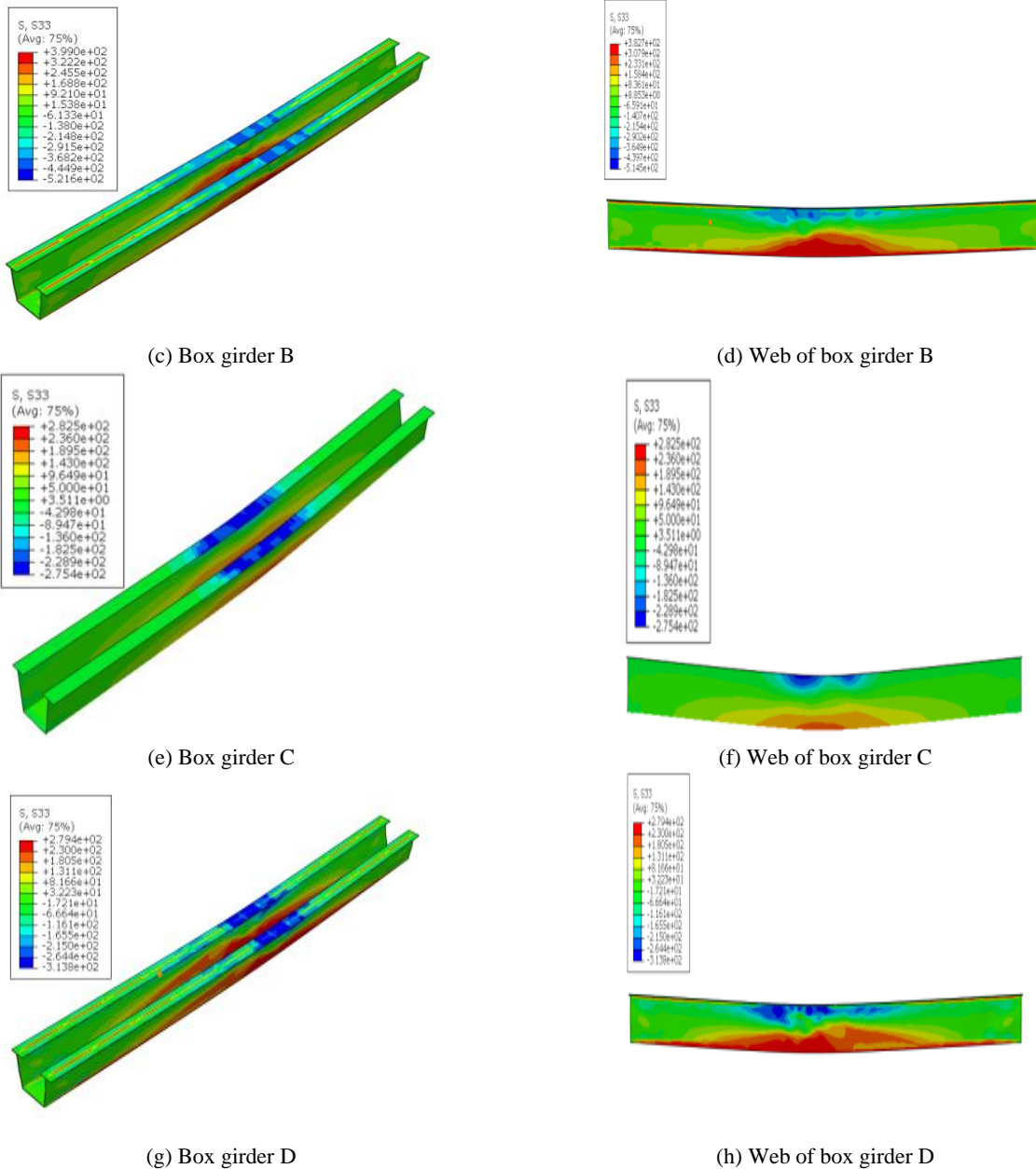


Figure 4. Failure states of different box girder.

#### 4. CONCLUSION

In this paper, based on the finite element software Abaqus, the welding temperature field of the aluminum alloy box girder is simulated, so as to study the stress change of the aluminum alloy box girder during the welding process. The results show that compared with the steel box girder, it is found that the impact of welding on the aluminum alloy box girder is more obvious, and its bearing capacity decreases by 24.94% after welding, and the steel box girder decreases by about 16.67% under the same conditions. When the aluminum alloy box girder reaches the ultimate bearing capacity, the failure mode is the same as that of the steel box girder, that is, bending failure.

## REFERENCES

- [1] Ueda, Y., Kim, Y, C. and Yuan, M, G., "A predicting method of welding residual stress using source of residual stress (report I)," *Journal of The Japan Welding Society*, 37(07), 39-43 (1989).
- [2] Ueda, Y., Murakawa, H. and Okumoto, Y., "Simulation of welding deformation for accurate ship assembling," *The Japan Society of Naval Architects and Ocean Engineers*, 1992(172), 559-566 (1992).
- [3] Bachorski, A., Painter, M, J. and Smailes, A, J., "Finite-element prediction of distortion during gas metal arc welding using the shrinkage volume approach," *Journal of Materials Processing Tech*, 92-93, 405-409 (1999).
- [4] Michaleris, P., Zhang, L. and Bhide, S, R., "Evaluation of 2D, 3D and applied plastic strain methods for predicting buckling welding distortion and residual stress," *Science and Technology of Welding and Joining*, 11(6), 707-716 (2006).
- [5] Deng, D., Murakawa, H. and Liang, W., "Numerical simulation of welding distortion in large structures," *Computer Methods in Applied Mechanics and Engineering*, 196(45-48), 4613-4627 (2007).
- [6] Sulaiman, M, S., Manurung, Y, H. and Haruman, E., "Simulation and experimental study on distortion of butt and T-joints using weld planner," *Journal of Mechanical Science and Technology*, 25(10), 2641-2646 (2011).
- [7] Chen, Z., Chen, Z, C. and Sheno, R, A., "Influence of welding sequence on welding deformation and residual stress of a stiffened plate structure," *Ocean Engineering*, 106, 271-280 (2015).
- [8] Bhatti, A, A., Barsoum, Z. and Murakawa, H., "Influence of thermo-mechanical material properties of different steel grades on welding residual stresses and angular distortion," *Materials and Design*, 65, 878-889 (2015).
- [9] Huang, H., Wang, J. and Li, L., "Prediction of laser welding induced deformation in thin sheets by efficient numerical modeling," *Journal of Materials Processing Tech*, 227, 117-128 (2016).